1 Computational Tools

1.1 MOOSE

Multiphysics Object-Oriented Simulation Environment (MOOSE)[3] is a computational framework whose purpose is to support engineering analysis applications. In a nuclear reactor, several partial differential equations (PDEs) describe its physical behavior. These equations are typically nonlinear, and they are often strongly coupled to each other. MOOSE targets such systems and solves them in a fully coupled manner.

MOOSE is an open-source code under a Lesser GNU Public License (LGPL). The code itself relies on LibMesh [4], an LGPL finite element library, and PetSc, a Berkeley Software Distribution (BSD)-licensed toolkit for solving nonlinear equations [1]. MOOSE applications define weak forms of the governing equations. They modularize the physics expressions into "Kernels." Kernels are C++ classes containing methods for computing the residual and Jacobian contributions of individual pieces of the governing equations. MOOSE and LibMesh translate them into residual and Jacobian functions. These functions become inputs into PetSc solution routines.

MOOSE utilizes the mathematical structure present in Jacobian-Free Newton-Krylov (JFNK) methods [5]. JFNK methods are synergistic combinations of Newton-type methods for superlinearly convergence of nonlinear equations and Krylov subspace methods for solving the Newton correction equations. The link between the two methods is the Jacobian-vector product. JFNK methods compute such products approximately without forming and storing the elements of the true Jacobian. The ability to perform a Newton iteration without forming the Jacobian gives JFNK methods potential for application throughout problems governed by nonlinear partial differential equations.

All the software built on the MOOSE framework shares a joint code base. The applications, by default, use monolithic and implicit methods. This feature facilitates relatively easy coupling between different phenomena and allows for great flexibility, even with a large variance in time scales [11]. Additionally, all codes use MPI for parallel communication and allow for deployment on massively-parallel cluster-computing platforms.

1.2 Moltres

Moltres [8] is a MOOSE based application initially designed for modeling fluid-fuelled Molten Salt Reactors (MSRs). This simulation tool is open source and counts with an LGPL license. It uses `git` for version control, emphasizing its openness and promoting quality through peer review.

Moltres solves arbitrary-group neutron diffusion, precursors, and temperature governing equations. It can solve the equations in a fully-coupled way or solve each system independently, allowing for great flexibility and making it applicable to a wide range of nuclear engineering problems.

2 Serpent

The Serpent Monte Carlo code [6] [7] is a three-dimensional continuous-energy neutron transport code. VTT Technical Research Centre of Finland developed it, and it has been in public distribution since 2009. Monte Carlo neutron transport codes have several reactor physics applications related to criticality safety analyses, radiation shielding problems, detector modeling, and validation of deterministic transport codes. The Monte Carlo method's main advantage is its capability to model geometry and interaction physics without significant approximations. The main disadvantage is that modeling complex systems are very computing-intensive, restricting the applications to some extent.

Serpent serves two primary purposes: (1) reactor modeling, and (2) group constant generation. In reactor modeling, the Monte Carlo simulation itself represents the solution to the full-scale problem. In group constant generation, the transport simulation produces input parameters for a deterministic code. Based on a few groups, deterministic codes allow for carrying out coupled full-core analyses.

In this work, Serpent produces group constants that serve as an input for Moltres and solves the heterogeneous system. This last step provides the reference solutions for the validation of the Moltres calculation scheme. For the calculations, we used Serpent 2.1.31 and the cross-section library JEFF3.1.2. The choice of Serpent as the cross-section generation tool comes from one of its capabilities. Serpent allows for the explicit modeling of randomly located TRISO particles. Applying a simple volume homogenization has proven inaccurate due to the resonant self-shielding effect of the kernel and coated layers. Although the particles' explicit modeling is time-consuming, costly, and impractical for most applications, it results necessary.

3 Mathematical Basis

3.1 Diffusion and precursors equations

Equations 1 and 2 describe the time dependent behavior of the neutronics.

$$\frac{1}{v_g}\frac{\partial}{\partial t}\phi_g = \nabla \cdot D_g \nabla \phi_g - \Sigma_g^r \phi_g + \sum_{g \neq g'}^{G} \Sigma_{g' \to g}^s \phi_{g'} + \chi_g^p \sum_{g'=1}^{G} (1-\beta) \nu \Sigma_{g'}^f \phi_{g'} + \chi_g^d \sum_{i}^{I} \lambda_i C_i \tag{1}$$

$$\frac{\partial}{\partial t} C_i = \sum_{g'=1}^{G} \beta_i \nu \Sigma_{g'}^f \phi_{g'} - \lambda_i C_i \tag{2}$$

where

$$\begin{aligned}
v_g &= \text{group } g \text{ neutron speed} \\
\phi_g &= \text{group } g \text{ neutron flux} \\
t &= \text{time} \\
D_g &= \text{group } g \text{ diffusion coefficient} \\
\Sigma_g^r &= \text{group } g \text{ macroscopic removal cross-section} \\
\Sigma_{g' \to g}^s &= \text{group } g' \text{ to group } g \text{ macroscopic scattering cross-section} \\
\chi_g^p &= \text{group } g \text{ prompt fission spectrum} \\
G &= \text{number of discrete energy groups} \\
\nu &= \text{number of neutrons produced per fission} \\
\Sigma_g^f &= \text{group } g \text{ macroscopic fission cross-section} \\
\chi_g^d &= \text{group } g \text{ delayed fission spectrum} \\
I &= \text{number of delayed neutron precursor groups} \\
\beta &= \text{delayed neutron fraction} \\
\lambda_i &= \text{average decay constant of delayed neutron precursors in precursor group } i \\
C_i &= \text{concentration of delayed neutron precursors in precursor group } i.
\end{aligned} \tag{3}$$

We apply the vacuum boundary condition to the diffusion equation. The vacuum boundary condition states that no neutrons penetrate the boundary in the inward direction. In other words, the incoming current density ($J^-(r_s,t)$) is equal to zero, equation 4 [2].

$$J^-(r_s,t) = \frac{1}{4}\phi(r_s,t) + \frac{D}{2}\hat{n_s} \cdot \nabla \phi(r_s,t) = 0 \tag{4}$$

3.2 Thermal-hydraulics

The governing equation for the temperature of the solids is the three-dimensional heat conduction equation [9]. Equations 5 to 7 allow for solving the temperature in the fuel, moderator, and reflector.

$$\rho_i c_{p,i} \frac{\partial}{\partial t} T_i = k_i \nabla^2 T_i + Q_i \tag{5}$$

$$Q_f = \sum_{g=1}^{G} \varepsilon_g^f \Sigma_g^f \phi_g \tag{6}$$

$$Q_m = Q_r = 0 \tag{7}$$

where

$$\begin{aligned} i &= \text{f (fuel), m (moderator), r (reflector)} \\ \rho_i &= \text{material } i \text{ density} \\ c_{p,i} &= \text{material } i \text{ heat capacity} \\ k_i &= \text{material } i \text{ thermal conductivity} \\ T_i &= \text{material } i \text{ temperature} \\ Q_i &= \text{material } i \text{ volumetric heat source} \\ \varepsilon_g^f &= \text{energy released per fission} \\ \Sigma_g^f &= \text{group } g \text{ macroscopic fission cross-section} \\ \phi_g &= \text{group } g \text{ neutron flux.} \end{aligned}$$

The governing equation of the coolant is the one-dimensional form of the continuity, momentum, and energy conservation equations, equations 8 to 12 [14][13].

$$\frac{\partial}{\partial t} \rho_c + \nabla \cdot (\rho_c u) = 0 \tag{8}$$

$$\rho_c \left(\frac{\partial}{\partial t} u + u \frac{\partial}{\partial z} u \right) = -\frac{\partial}{\partial z} p - \tau \frac{\varepsilon}{A} - \rho_c g \tag{9}$$

$$\rho_c \left(\frac{\partial}{\partial t} (c_{p,c} T_c) + u \frac{\partial}{\partial z} (c_{p,c} T_c) \right) = \frac{\partial}{\partial t} p + u \frac{\partial}{\partial z} p + q'''_{conv} \tag{10}$$

$$\tau = \frac{f}{2} \rho_c u^2 \tag{11}$$

$$q'''_{conv} = h \frac{\varepsilon}{A} (T_i - T_c) \tag{12}$$

where

ρ_c = coolant density
u = coolant velocity
p = coolant pressure
τ = shear stress
ε = wetted perimeter
A = cross-sectional area
g = gravity
$c_{p,c}$ = coolant specific heat capacity
T_c = coolant temperature
k_c = coolant thermal conductivity
q'''_{conv} = convective heat transfer
f = friction factor
h = heat transfer coefficient
T_i = solid temperature.

4 OECD/NEA MHTGR-350 MW Benchmark

The deterministic neutronic thermal-fluids and transient analysis methods available for prismatic High Temperature Gas-Cooled Reactors (HTGRs) have lagged behind the state of the art of other reactor technologies. This delay has motivated the development of more accurate tools for the design and safety evaluations of HTGRs. In addition to the development of new methods, it is essential to define appropriate benchmarks to compare these new methods' capabilities. The Organisation for Economic Co-operation and Development (OECD)/Nuclear Energy Agency (NEA) defined such a benchmark [10] using the Modular High-Temperature Gas-Cooled Reactor (MHTGR)-350 MW reactor [12] as the reference design. The scope of the benchmark is twofold: (1) to establish a well-defined problem, based on a common given data set, to compare methods and tools in core simulation and thermal fluids analysis, and (2) to test the depletion capabilities of various lattice physics codes available for prismatic HTGRs.

The benchmark defines several Phases and Exercises:

- Phase I: Steady State
    1. Neutronics solution with fixed cross-sections.
    2. Thermal fluids solution with given heat sources.
    3. Coupled neutronics-thermal fluids steady state solution.
- Phase II: Transient Cases
    1. Depressurized Conduction Cooldown without reactor trip.
    2. Pressurized Conduction Cooldown with reactor trip.
    3. Water ingress with reactor trip.
    4. Power 100-80-100 load follow.
- Phase III: Lattice Depletion Case

5 MHTGR-350 Reactor Description

This section describes the MHTGR-350 reactor. Table 1 lists its main characteristics. The core consists of an array of hexagonal fuel elements in a cylindrical arrangement, Figure 1. Nineteen graphite replaceable reflector elements compose the inner reflector region. A ring of identically sized graphite replaceable reflector elements surrounds the fuel elements. Then, a region of permanent reflector elements follows the replaceable reflectors. The reactor vessel encases all the elements.

Table 1: MHTGR350 Characteristics [10].

Characteristics	Value
Installed Thermal Capacity	350 MWt
Installed Electric Capacity	165 MWe
Core inlet/outlet Temperature	259/687°C
Power Density	5.9 MW/m^3
Reactor Vessel Outside diam.	6.8 m
Reactor Vessel Height	22 m
Active core radius	2.97 m
Active core height	7.93 m
Top reflector height	1.20 m
Bottom reflector height	1.60 m
Number of fuel columns	66
Number of inner reflector columns	19
Number of outer reflector columns	78

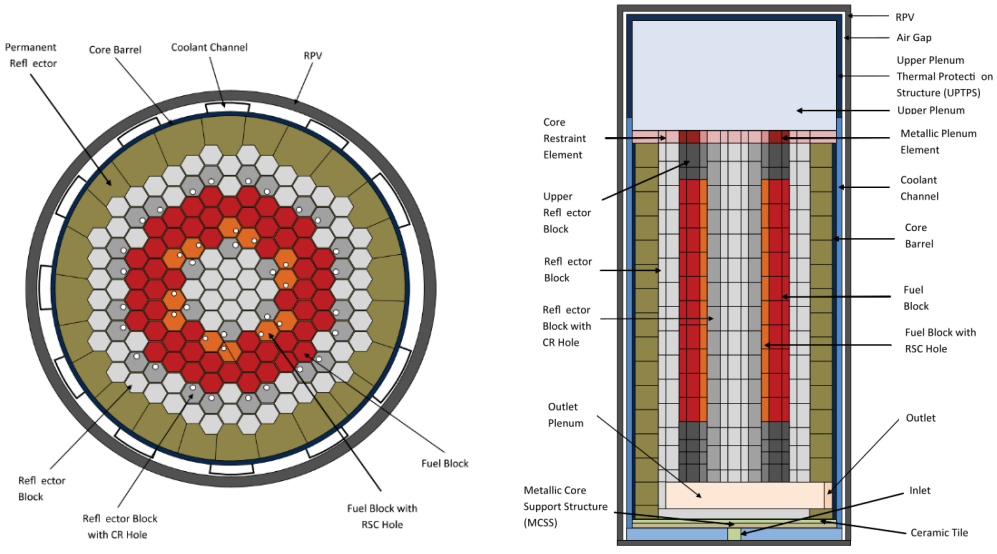

(a) Core radial layout. Image reproduced from [10].

(b) Core axial layout. Image reproduced from [10].

Figure 1: MHTGR reactor layout.

Ten layers of fuel elements stacked on top of each other compose the 66 fuel columns that integrate the active core. Figure 1b shows an axial view of the reactor. The core has two types of fuel elements: a standard element and a reserve shutdown element that contains a channel for Reserve Shutdown Control (RSC). Table

2 specifies the details of the MHTGR-350 fuel elements. Twelve columns in the core contain RSC channels for reserve shutdown borated graphite pellets. Hoppers above the core house the pellets, and if the control rods (CRs) become inoperable, the pellets drop into the channels [10].

Table 2: MHTGR350 fuel element characteristics [10].

Shared characteristics	Value	Units
Block pitch (flat-to-flat)	36	cm
Fuel length	79.3	cm
Fuel handling diameter	3.5	cm
Fuel handling length	26.4	cm
RSC hole diameter	9.525	cm
RSC center to assembly center	9.756	cm
Fuel/coolant pitch	1.879	cm
Fuel hole radius	0.635	cm
Compacts per fuel hole	15	-
Large coolant hole radius	0.794	cm
Small coolant hole radius	0.635	cm
LBP hole radius	0.635	cm
Block graphite density	1.85	g/cm^3
Standard element		
Number of large coolant holes	120	-
Number of small coolant holes	6	-
Number of fuel holes	210	-
RSC element		
Number of large coolant holes	88	-
Number of small coolant holes	7	-
Number of fuel holes	186	-

The fuel elements contain blind holes for fuel compacts and full-length channels for helium coolant flow. Table 3 specifies the details of the TRISO particle and fuel compact designs of the MHTGR-350.

A combination of Lumped Burnable Poison (LBP) and CRs controls the core reactivity. The LBP consists of boron carbide (B4C) granules dispersed in graphite compacts. The current design uses six LBP rods per element. Table 4 displays the characteristics of the LBP compacts. The reactor counts with 30 CRs. Six of them are start-up CRs, and their location is the inner reflector. The remaining 24 are operating CRs and control the reactivity during power operation and a reactor trip.

Table 3: TRISO and fuel compact characteristics [10].

Characteristic	Value	Units
Fuel	$UC_{0.5}O_{1.5}$	-
Enrichment (average)	15.5	wt%
Packing fraction (average)	0.35	-
Kernel radius	0.02125	cm
Buffer radius	0.03125	cm
IPyC radius	0.03475	cm
SiC radius	0.03825	cm
OPyC radius	0.04225	cm
Compact radius	0.6225	cm
Compact gap radius	0.6350	cm
Compact length	4.9280	cm
Kernel density	10.50	g/cm^3
Buffer density	1.00	g/cm^3
IPyC density	1.90	g/cm^3
SiC density	3.20	g/cm^3
OPyC density	1.90	g/cm^3
Compact matrix density	1.74	g/cm^3

Table 4: LBP compact characteristics [10].

Characteristic	Value	Units
Absorber	B_4C	-
Packing fraction	0.109	-
Kernel radius	0.0100	cm
Buffer radius	0.0118	cm
PyC radius	0.0141	cm
Compact radius	0.5715	cm
Compact gap radius	0.6350	cm
Rod length	72.187	cm
Kernel density	2.47	g/cm^3
Buffer density	1.00	g/cm^3
PyC density	1.87	g/cm^3
Compact matrix density	0.94	g/cm^3

References

[1] Balay, Brune, Buschelman, Gropp, Karpeyev, Knepley, Curfman McInnes, Rupp, Smith, and Zhang. PETSc Users Manual, April 2016.

[2] James J. Duderstadt and Louis J. Hamilton. *Nuclear Reactor Analysis*. Wiley, New York, 1 edition edition, January 1976.

[3] Derek Gaston, Chris Newman, Glen Hansen, and Damien Lebrun-Grandié. MOOSE: A parallel computational framework for coupled systems of nonlinear equations. *Nuclear Engineering and Design*, 239(10):1768–1778, October 2009.

[4] Benjamin S. Kirk, John W. Peterson, Roy H. Stogner, and Graham F. Carey. libMesh : a C++ library for parallel adaptive mesh refinement/coarsening simulations. *Engineering with Computers*, 22(3-4):237–254, December 2006.

[5] D.A. Knoll and D.E. Keyes. Jacobian-free Newton–Krylov methods: a survey of approaches and applications. *Journal of Computational Physics*, 193(2):357–397, January 2004.

[6] Jaakko Leppänen. Development of a New Monte Carlo Reactor Physics Code. page 241, June 2007.

[7] Jaakko Leppänen, Manuele Aufiero, Emil Fridman, Reuven Rachamin, and Steven van der Marck. Calculation of effective point kinetics parameters in the Serpent 2 Monte Carlo code. *Annals of Nuclear Energy*, 65:272–279, March 2014.

[8] Alexander Lindsay, Gavin Ridley, Andrei Rykhlevskii, and Kathryn Huff. Introduction to Moltres: An application for simulation of Molten Salt Reactors. *Annals of Nuclear Energy*, 114:530–540, April 2018.

[9] Gilbert Melese and Robert Katz. *Thermal and flow design of helium-cooled reactors*. American Nuclear Society, La Grange Park, Ill., USA, 1984.

[10] OECD NEA. Benchmark of the Modular High-Temperature Gas-Cooled Reactor (MHTGR)-350 MW Core Design Volumes I and II. page 110, 2017.

[11] A J Novak, L Zou, J W Peterson, R C Martineau, and R N Slaybaugh. Pronghorn: A Porous Media Thermal-Hydraulics Core Simulator and its Validation with the SANA Experiments, April 2018.

[12] F. Silady, J. Cunliffe, and L. Walker. The Licensing Experience of the Modular High-Temperature Gas-Cooled Reactor (MHTGR), September 1988.

[13] Tak, Kim, Lim, and Noh. A practical method for Whole-Core Thermal Analysis of a Prismatic Gas-Cooled Reactor, March 2012.

[14] F White. *Viscous Fluid Flow*. McGraw Hill, third edition, 2006.